Combustion stabilization using serpentine plasma actuators

Chin-Cheng Wang and Subrata Roy[a)]
Applied Physics Research Group, Department of Mechanical and Aerospace Engineering, University of Florida, Gainesville, Florida 32611-6300, USA

(Received 26 May 2011; accepted 27 June 2011; published online 28 July 2011)

This letter presents a numerical model for combustion stabilization with plasma actuators. Recently, we demonstrated that serpentine actuators induce complex neighboring flow structures due to pinching and spreading effects suitable for rapid flow mixing. Here, the influence of serpentine plasma actuator is numerically investigated on inner and outer recirculation zones of a gas turbine combustor. Beyond benchmarking with reported experimental data, we show that the swirl generated by the serpentine plasma actuators creates local low velocity regions stabilizing the flame. Such simple flow-mixing device does not need any moving parts, hence may be useful in the any combustors. © *2011 American Institute of Physics*. [doi:10.1063/1.3615292]

The topic of plasma assisted combustion (PAC) has been investigated in recent years.[1] Leonov and Yarantsev[2] reported that there are at least four possible mechanisms of PAC such as momentum transfer in electric and magnetic fields. Our recent publications[3,4] numerically predicted and experimentally demonstrated that the serpentine dielectric barrier discharge (DBD) actuator instills inherent three-dimensional flow instabilities that can influence beyond the flow boundary layer. It not only induces rapid transitional mixing but also extracts momentum from an upstream flow injecting it into the bulk fluid. In the present study, we introduce these electrically driven serpentine actuators[4] to improve flame stability by inducing recirculation regions for a class of gas turbine combustors. We anticipate that these actuators will advance the state-of-the-art for flow mixing. Applications include bluff bodies and passive swirl generators for combustors.[5–7]

The effect of electric fields on flames has been shown to improve flame stabilization of lean mixtures. Schmidt *et al.*[8] showed millisecond pulsed plasma has an overall effect of slowing gas-flow speed in the flame replicating a virtual bluff body. Chintala *et al.*[9] presented the results of RF discharge experiments in premixed combustible mixtures and demonstrated flame stabilization. Anikin *et al.*[10] presented that a pulsed nanosecond barrier discharge allows a twofold increase of the blow-off velocity consuming less than 1% from the burner power. In summary, it has been shown through experiments that plasma can improve flame stabilization and sufficiently increase combustion efficiency.

This letter focuses on the improvement of flame stabilization through serpentine plasma actuators. Figure 1 shows schematic of a gas turbine combustor from Weigand *et al.*[11] that as been modified with serpentine plasma actuators on the front and back walls. The actuators are installed at $y = \pm 42.5$ mm and $z = 10$ mm. Here, the electrodes which are separated by a dielectric do not contain any mechanical parts and can be surface compliant. Appropriate designing of such plasma actuators can help three-dimensional flow mixing.[3,4] The combustor setup shown in Figure 1 is for counter-flow electrode arrangement which induces plasma force opposing the flow direction. The geometry of the serpentine actuator is also described in the inlay of Figure 1. The width of the electrodes and the gap between electrodes were fixed at 2 mm. Details of this serpentine actuator can be found in our previous publication.[4] The thick purple arrows show the plasma force vectors against the incoming fresh air. In contrast, for the case of co-flow serpentine, the actuators have been rotated 180° to actuate the incoming fresh air in the same axial (z) direction. There are two air nozzles (central and annular)[11] swirling air in the same direction. The incoming co-swirling air (O_2) is supplied from a plenum through the annular ($D_i = 17$ mm; outer $D_o = 25$ mm) and central ($D = 15$ mm) nozzles. The non-swirling methane fuel (CH_4) is injected through 72 channels (0.5×0.5 mm^2) into the combustion chamber between two air nozzles. The combustion chamber had a square section of 85×85 mm^2 and a height of 110 mm. The chamber is connected by a top plate to the central exit at 40 mm. We numerically test the system prescribed as "flame A" in Ref. 11 for stable combustion as our benchmark case to show the effect of serpentine plasma actuators. We also explore how

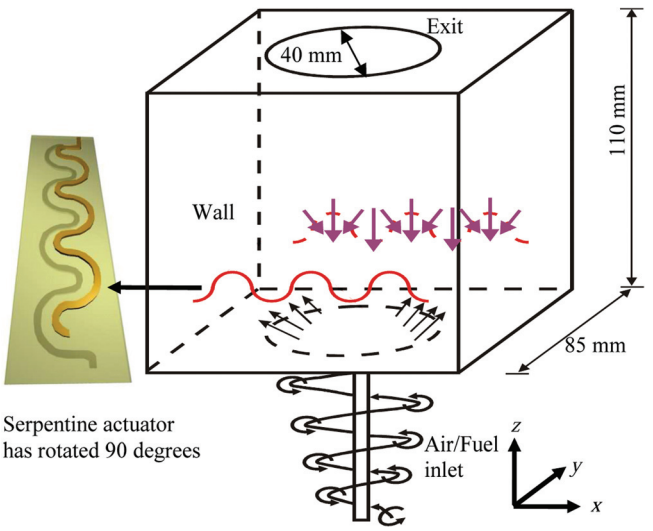

FIG. 1. (Color) Schematic of the gas turbine combustor with serpentine plasma actuators.

[a)]Electronic mail: roy@ufl.edu.

 © 2011 American Institute of Physics

the serpentine distribution of plasma force may stabilize non-premixed turbulent combustion.

To reduce the numerical complexity, we employ first-principles calculation of the plasma body force distribution from our recent study[4] computed using our in-house parallelized modular multiscale ionized gas (MIG) flow code. The effect of plasma actuation is incorporated into the Navier-Stokes flow equations through the time-averaged electric force density, $F_j = \frac{1}{m}[\Sigma_{i=1}^{m} e(N-n)E_j]$, where $j = x,y,z$ direction, e is the elementary charge, E is the electric field, N is the ion number density and n is the electron number density, and $m = 40$ is the number of time stations in a cycle used for time-averaging. A commercial flow solver, FLUENT, is used for combustion simulation where F_j force is incorporated as a source term in the momentum equations via user defined functions (UDF). The numerical model of reacting flows is governed by the averaged conservation equations[5] for mass fraction, momentum, chemical species, and energy. For unity Lewis number, a one-step global reaction mechanism is used for methane/air combustion. The single irreversible reaction equation is described as $CH_4 + 2O_2 \rightarrow CO_2 + 2H_2O$. The eddy-dissipation model that provides a turbulence-chemistry interaction is chosen for calculating the single step heat release mechanism.

The computational domain is $85 \times 85 \times 110$ mm^3 for the reacting flows. A three-dimensional hexahedral mesh of $110 \times 110 \times 125$ cells is created for the combustion chamber. The mesh quality is maintained within the maximum aspect ratio of 10 and the skewness less than 0.5. The cell size close to the flame base is ranged from 0.8 to 0.1 mm, which is sufficient to resolve the turbulence length scales. For the benchmark case, we impose the experimental data[11] corresponding to Reynolds number of 58 000 at the inlet boundary ($z = 1.5$ mm) and assume zero gauge pressure at the exit. All other boundaries are assumed to be no-slip wall condition. For the cases of plasma assisted combustion, we test three cases which are (1) baseline with no plasma, (2) co-flow serpentine plasma actuation, and (3) counter-flow serpentine plasma actuation. The serpentine plasma force distribution obtained from our prior publication[4] is interpolated into Navier-Stokes solver as UDF of local body source terms. It has been experimentally proved that the averaged power consumption of the serpentine plasma actuator is ~4.8 W.[4] In this letter, the employed plasma force density is on the order of hundreds of kN/m^3. Such plasma force may be obtained by using hundreds of watts. While dielectric barrier discharge actuators may not be sufficiently strong for this augmentation, local high-frequency (100 kHz) nanosecond pulse surface discharge may be a possible solution.[12]

For the benchmark case, Figure 2 shows the comparison of experiment[11] (left) and simulation (right) of time-averaged velocity vector plots at the central plane ($x = 0$) of the combustion chamber. Here, we can see very similar flow characteristics of the inner recirculation zone (IRZ) at the center and the outer recirculation zone (ORZ) near the wall in both experiment and simulation. The velocity vectors colored by black represent positive axial velocity, while the negative axial velocities are displayed in red. For this type of confined swirl flame, IRZ ensures the mixing of the fuel with air, while ORZ mixes hot burned products into reactants near

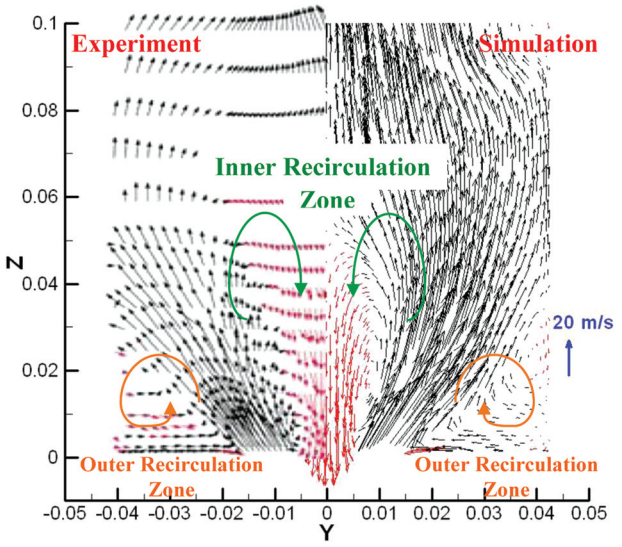

FIG. 2. (Color) Comparison of experiment and simulation of time-averaged velocity vectors colored by axial velocity; negative axial velocities are displayed in red.

the flame base. Both experiment and simulation have almost the same jet angle of maximum mean velocity of ~26° with respect to the axial centerline. Also, the center of recirculation regions are located at the same height of $z = 22.5$ mm for both IRZ and ORZ.

Figure 3 shows the comparison of experiment[11] (dots) and simulation (solid lines) of time-averaged velocity components from the center ($y = 0$) to the wall ($y = 42.5$ mm) at $z = 5$. The numerical results of velocity components are in good agreement with previously reported experimental data.[11] At $z = 5$ mm, the positive maximum peak of 37 m/s and the negative minimum peak of −23 m/s in the axial velocity denote the inflow of the fresh gas and the inner recirculation zone, respectively. The simulated highest time-averaged axial velocity is close to the experimental data of 38 m/s. The radial velocity is negative for $y > 20$ mm representing the size of the ORZ. The maximum peak of the mean radial velocity in the IRZ is almost twice the size of that in the ORZ. For the tangential velocity, it seems rather flat (~11.5 m/s) in the ORZ. In the IRZ, we can see two humps reflecting the swirling air from annular and central nozzles.

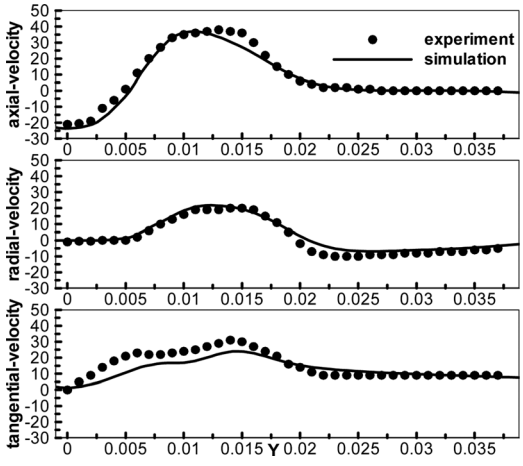

FIG. 3. Radial profiles of time-averaged axial, radial, and tangential velocity distributions at $z = 5$ mm.

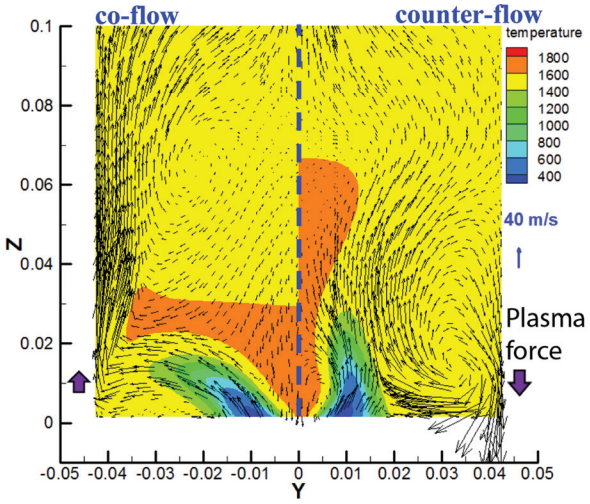

FIG. 4. (Color) Velocity vector plots of co-flow serpentine (left) and counter-flow serpentine (right) plasma actuation.

Our simulated tangential velocity captures the trends of these two humps well in the IRZ.

Figure 4 describes velocity vector and temperature contour plots for co-flow (left) and counter-flow (right) serpentine plasma actuation on the side walls ($y = \pm 42.5$ mm; $z = 10$ mm) of the combustion chamber. For the co-flow serpentine plasma actuator, it pinches and spreads fresh air in the vicinity of troughs and crests, respectively. Such plasma actuation (or disturbance) enhances mixing of the surrounding fuel with air. In comparison to baseline (or benchmark) case shown in Figure 2, the size of the IRZ ($y = \pm 30$ mm; $z = 70$ mm) of the co-flow serpentine case is much bigger than baseline case. Furthermore, the bigger IRZ means the wider low velocity region to stabilize the flame at the center. Conversely, if the IRZ becomes too small, it may cause combustion instability. For the counter-flow serpentine case, two large ORZ are created near the walls to mix the cold incoming fresh air with hot burned gas. Apparently, the size of the ORZ ($y = \pm 20$ to ± 42.5 mm; $z = 50$ mm) of counter-flow serpentine is wider than the baseline and co-flow serpentine cases. However, the large ORZ from the walls may squeeze the size of the IRZ at the center. So the combustion may become unstable due to less residence time to anchor the flame at the base. Figure 5 plots radial profiles of velocity and temperature components for the cases of baseline, co-flow serpentine, and counter-flow serpentine at $z = 15$ mm. At $z = 15$ mm, both co-flow serpentine and counter-flow serpentine have considerable changes in the velocities. For the co-flow serpentine, the axial velocity in the IRZ is much lower than other cases indicating that more residence time is available. Specially, the counter-flow serpentine produces the strongest swirl (i.e., tangential velocity) in the IRZ, while the co-flow serpentine leads to the largest swirl in the ORZ.

All three cases exhibit similar trends which start the highest temperature then decrease the lowest temperature and then rise to 1600 K. The low temperature region ($y = 5-25$ mm) reflects the incoming cold swirl air, while the high temperature region is mainly due to the enhancement of flow mixing. For the co-flow serpentine, the wider IRZ is able to increase the residence time in the low temperature region (i.e., cold fresh air). In contrast, for the counter-flow serpentine, the

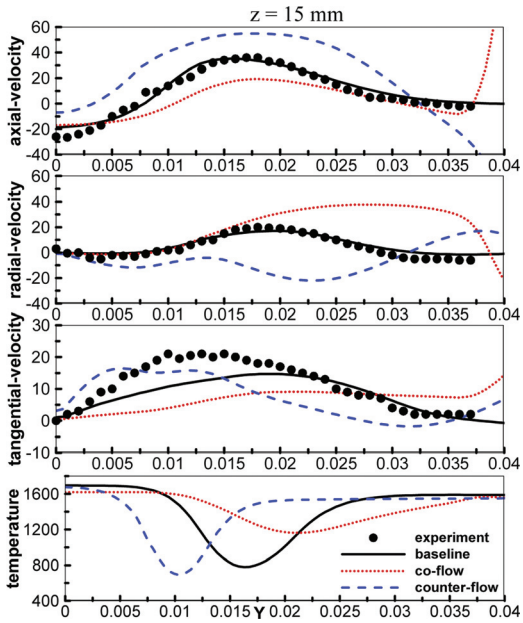

FIG. 5. (Color) Radial profiles of time-averaged axial, radial, and tangential velocity distributions for the baseline, co-flow serpentine and counter-flow serpentine at locations of $z = 15$ mm.

larger ORZ mixes hot products into reactants and then increase the combustion temperature. However, the increasing ORZ near the walls may squeeze the size of IRZ at the center.

In conclusion, numerical studies of three-dimensional plasma assisted reacting flows are performed. Numerical results for the benchmark case compared well with experimental data. For the cases of co-flow and counter-flow serpentine, our results demonstrate that serpentine actuators can significantly influence the combustion process by creating a large IRZ/ORZ enhancing the mixing of the surrounding fuel with air. The co-flow serpentine actuator creates larger IRZ than the baseline (no plasma) case predicting better flame stabilization. Such low power flow-mixing devices may be useful for the replacement of the air swirlers. This research may benefit the design of plasma assisted gas turbine combustor. Experiment is on the way to validate our numerical results of plasma assisted combustion.

[1]S. M. Starikovskaia, J. Phys. D: Appl. Phys. **39**, R265 (2006).
[2]S. B. Leonov and D. A. Yarantsev, Plasma Sources Sci. Technol. **16**, 132 (2007).
[3]S. Roy and C. C. Wang, J. Phys. D: Appl. Phys. **42**, 032004 (2009).
[4]C. C. Wang, R. J. Durscher, and S. Roy, J. Appl. Phys. **109**, 083305 (2011).
[5]T. Poinsot and D. Veynante, *Theoretical and Numerical Combustion* (Edwards, Philadelphia, 2005), p. 141.
[6]A. K. Gupta, D. G. Lilley, and N. Syred, *Swirl Flows* (Abacus, Yunbridge Wells, UK, 1984), p. 1.
[7]S. R. Turns, *An Introduction to Combustion: Concepts and Applications* (McGraw-Hill Higher Education, Columbus, OH, 2000), p. 470.
[8]J. B. Schmidt, S. Kostka, A. C. Lynch, *et al.*, 49th AIAA Aerospace Sciences Meeting, Orlando, FL, 2011, Paper No. 2011-1021.
[9]N. Chintala, R. Meyer, and I. Adamovich, 42nd AIAA Aerospace Sciences Meeting and Exhibit, Reno, NV, 2004, Paper No. 2004-0835.
[10]N. B. Anikin, E. I. Mintoussov, S. V. Pancheshnyi, *et al.*, 41st AIAA Aerospace Sciences Meeting and Exhibit, Reno, NV, 2003, Paper No. 2003-1053.
[11]P. Weigand, W. Meier, X. R. Duan, *et al.*, Combust. Flame **144**, 205 (2006).
[12]M. Nishihara, K. Takashima, J.W. Rich, *et al.*, 49th AIAA Aerospace Sciences Meeting, Orlando, FL, 2011, Paper No. 2011-1144.